J Nanopart Res (2015) 17:476
DOI 10.1007/s11051-015-3290-0

RESEARCH PAPER

Tannic acid- and natural organic matter-coated magnetite as green Fenton-like catalysts for the removal of water pollutants

C. Nadejde · M. Neamtu · V.-D. Hodoroaba · R. J. Schneider · A. Paul · G. Ababei · U. Panne

Received: 23 August 2015 / Accepted: 30 November 2015 / Published online: 11 December 2015

Abstract The use of magnetic materials as heterogeneous catalysts has attracted increasing attention in the last years since they proved to be promising candidates for water treatment. In the present study, two types of surface-modified magnetite (Fe_3O_4) nanoparticles, coated with non-hazardous naturally occurring agents—either tannic acid (TA) or dissolved natural organic matter—were evaluated as magnetic heterogeneous catalysts. Chemical synthesis (co-precipitation) was chosen to yield the nanocatalysts due to its well-established simplicity and efficiency. Subsequently, the properties of the final products were fully assessed by various characterization techniques. The catalytic activity in heterogeneous oxidation of aqueous solutions containing a model pollutant, Bisphenol A (BPA), was comparatively studied. The effect of operational parameters (catalyst loading, H_2O_2 dosage, and UV light irradiation) on the degradation performance of the oxidation process was investigated. The optimum experimental parameters were found to be 1.0 g/L of catalysts and 10 mM H_2O_2, under UV irradiation. The highest mineralization rates were observed for Fe_3O_4-TA catalyst. More than 80 % of BPA was removed after 30 min of reaction time under the specified experimental conditions. The obtained results showed that the two catalysts studied here are suitable candidates for the removal of pollutants in wastewaters by means of heterogeneous reaction using a green sustainable treatment method.

Keywords Nanocatalysts · Characterization · Photo-Fenton oxidation · Wastewater · Bisphenol A degradation · Environment · Mitigation

C. Nadejde (✉) · M. Neamtu (✉)
Interdisciplinary Research Department – Field Science, 'Alexandru Ioan Cuza' University, Lascar Catargi Str. 54, 700107 Iasi, Romania
e-mail: claudianadejde@gmail.com

M. Neamtu
e-mail: mariana.neamtu@uaic.ro

V.-D. Hodoroaba · R. J. Schneider · A. Paul · U. Panne
BAM Federal Institute for Materials Research and Testing, Unter den Eichen 87, 12205 Berlin, Germany

G. Ababei
National Institute of Research and Development for Technical Physics, Dimitrie Mangeron Blvd. 47, 700050 Iasi, Romania

U. Panne
Department of Chemistry, Humboldt-Universität zu Berlin, Brook-Taylor-Str. 2, 12489 Berlin, Germany

Introduction

Over the last years, the increasing concentration of micropollutants in waters and soil, originating from human activity, became a major threat to environmental ecosystems. Since clean water sources are rapidly diminishing, while environment pollution already is an issue of great concern, novel greener

alternatives for water decontamination are continuously sought for better management of water treatment (Nowack 2008; Chong et al. 2010; Qu et al. 2013). To date, most water treatment technologies used for pollutants' removal are either time consuming or requiring high operating costs; advanced oxidation processes (AOP), such as photo-Fenton oxidation, have proved to be better approaches for degradation of contaminants in waters due to the increased oxidation efficiency using a simple technology under mild reaction conditions (Gilmour 2012).

The use of magnetic nanoparticles as heterogeneous catalysts in water decontamination for efficient mineralization of persistent micropollutants has attracted increasing attention in the last years (Ren et al. 2013; Shahwan et al. 2011; Sun and Lemley 2011; Munoz et al. 2015; Nadejde et al. 2015; Hanif and Shahzad 2014; Song et al. 2013). Magnetite (Fe_3O_4) nanoparticles represent promising candidates as catalysts during AOP due to their benign nature, low-cost, simple, and large-scale manufacturing (Munoz 2015; Nadejde et al. 2015; Wang et al. 2012; Zhang et al. 2008, 2009; Atacan and Özacar 2015); furthermore, their properties can be tailored according to their purpose; the nanostructures' surface can be functionalized with a wide variety of non-toxic materials containing (photo)active groups that act both as nanoparticle stabilizers and also as catalysts. Moreover, their activity and selectivity are strongly dependent on the catalyst physico-chemical properties. The magnetic properties of such nanoscale systems allow their facile re-collection from water (by applying an external magnetic field) and possible re-use in the next cycle of water treatment (Wang and Astruc 2014). All these advantages significantly contribute to reducing costs and increasing availability for large-scale applications.

Naturally occurring polymers, such as tannic acid (TA) and dissolved natural organic matter (NOM), are high-molecular weight polyphenolic compounds, widely spread, safe, and inexpensive natural materials, with high content of hydroxyl groups in their structure, well known for their strong interaction with iron. Thus, in the present study, TA and NOM were the coating agents of choice for stabilizing magnetic iron oxide nanoparticles (fabricated by co-precipitation method), in order to yield active Fenton-like nanocatalysts for the removal of persistent contaminants from waters.

Although other studies reported the use of similar type of nanomaterials in the degradation of dye pigments or adsorption of heavy metals from water (Genuino et al. 2013; Peng et al. 2012; Liu et al. 2008; Shahwan et al. 2011), the knowledge on their performance in the removal of non-biodegradable organic micropollutants such as endocrine disruptors (i.e., Bisphenol A) is limited. Due to its chemical structure, BPA was considered a synthetic estrogen-like compound for decades. Nowadays, BPA, used as a raw material for polycarbonate and epoxy resins, is known to accumulate in nature without decomposition and has been classified as an endocrine disruptive chemical (Neamtu et al. 2014). Significant amounts of BPA are continuously released in environment from various sources, the harmful effects on living organisms' health being well established (Virkutyte et al. 2010).

Therefore, the objective of this study is to investigate the properties and catalytic activity of the above-mentioned nanomaterials in heterogeneous oxidation of aqueous solutions containing BPA; the effects of reaction conditions—catalyst loading, H_2O_2 dosage, and UV irradiation—on the degradation efficiency of the oxidation process are further discussed.

Experimental

Materials

The catalyst synthesis procedures were performed using high-purity reagents (Sigma-Aldrich), while the dissolved NOM was isolated from surface water (Fuchskuhlelake, Brandenburg, Germany), up-concentrated by reverse osmosis, and later freeze-dried. Deionized water (18.2 MΩ/cm), obtained with Barnstead EASYpure™ II Ultrapure Water System, was used throughout the experiments.

Catalyst synthesis

The magnetic nanocatalysts were fabricated by employing a facile cost-effective synthesis procedure (chemical co-precipitation method). Briefly, the iron oxide (Fe_3O_4) magnetic nanoparticles were obtained by thoroughly mixing together ferric and ferrous salt precursors (2:1 stoichiometric ratio) in the presence of

a strong alkaline precipitation agent (1.7 M NaOH); the method was performed at a relatively high temperature (80 °C) with continuous stirring, under normal atmospheric conditions. The as-obtained magnetic black precipitate was subsequently purified by repeated rinsing with water and absolute ethanol, then coated with either TA or NOM, taking into consideration a molar ratio of 0.05 between the magnetic core and stabilizing shell. After 2 h of mechanical vigorous stirring at 40 °C, the samples were separated from suspension, repeatedly washed with water and absolute ethanol (in order to remove impurities and excess coating material), and then dried in a vacuum oven at ~40 °C. The choice of the capping agents was motivated by the fact that both tannic acid and NOM are non-toxic and inexpensive polymers, widely and naturally occurring in the environment, which have the ability not only to form strong complexes with iron but also to prevent particle oxidation and aggregation while ensuring excellent stability in time of such structures.

Catalyst characterization

The nanocatalysts were fully characterized by X-ray diffraction (XRD, Shimadzu LabX XRD-6000 X-ray diffractometer with Cu Kα radiation ($\lambda = 1.5418$ Å)), nitrogen adsorption–desorption isotherms and the Brunauer–Emmett–Teller (BET) tests (Micromeritics ASAP 2020^{TM} Physisorption system-Norcross, USA at 77 K), energy-dispersive X-ray spectroscopy (EDX, Bruker XFlash® 5030 SDD X-ray spectrometer with silicon drift detector-Berlin, Germany), high-resolution scanning electron microscopy (SEM, Supra 40 Carl Zeiss-Oberkochen, Germany) and high-resolution transmission electron microscopy (HRTEM) with selected area electron diffraction (SAED) (Zeiss Libra 200 MC TEM/STEM electron microscope operating at 200 kV), Fourier transform infrared spectroscopy (FTIR, Jasco 660 Plus spectrometer, KBr disk, 4 cm^{-1} resolution), and vibrating sample magnetometry (VSM, MicroMag Model 2900/3900 magnetometer, at room temperature).

Kinetic experiments

For the kinetic tests, the BPA aqueous solutions were prepared by adding an appropriate volume of stock solution to ultrapure water in order to reach the studied concentrations. The oxidation experiments (without UVA irradiation) were performed on a rotator SB3 (VWR International, Germany); the photo-oxidation tests were conducted using an orbital shaker Heidolph Titramax 100 with continuous mixing. The initial pH of the BPA solution was 6.6 without further adjusting. No BPA removal by adsorption on the catalysts was noticed during the heterogeneous (photo-)oxidation experiments. Two H_2O_2 concentrations (10 and 20 mM), prepared from a 30 % H_2O_2 initial solution, were tested during the Fenton-like oxidation experiments.

The photochemical experiments were carried out using UVA type xenon lamps (ATLAS Material Testing Solution, Germany) with an UV intensity of 40 W m^{-2} in the $290 \leq \lambda \leq 400$ nm range and a 1.4 cm irradiation path length; the photon flow (2.13×10^{-7} Einstein s^{-1}) of the solar UV simulator was measured by polychromatic actinometry with phenylglyoxylic acid in AcN:H_2O = 3:1 (v/v) (Defoin et al. 1986). In all experiments, the diameter of the irradiated surface area was 9.62 cm^2 for a total reaction volume of 8 mL.

Samples were withdrawn from the reaction medium regularly followed by immediate filtering through a 0.22 μm Teflon membrane filter for HPLC analysis. The sample analysis was carried out by HPLC–MS/MS (1100 HPLC workstation Agilent Technologies, Waldbronn, Germany, coupled to an API 4500 TSQ triple-stage quadrupole mass spectrometer ABSciex, Darmstadt, Germany); the procedure is presented in detail in our previous study (Nadejde et al. 2015).

Results and discussion

High-resolution SEM (Fig. 1a, b) and TEM (Fig. 1c, d) were employed in order to assess the morphology of the samples, surface, and the size of the primary particles.

The SEM micrographs show, as expected, nanoparticle chains of quasi-spherical shape having sizes between 10 and 25 nm; the results are in agreement with the ones obtained by HRTEM.

The high-magnification TEM images evidence the thin surrounding layer of the coating material (Fig. 1c, d). The SAED patterns (Fig. 1e, f) confirm that the magnetite cores are polycrystalline surrounded by the amorphous structure of the coating agents, which is revealed by the presence of the small spots on the

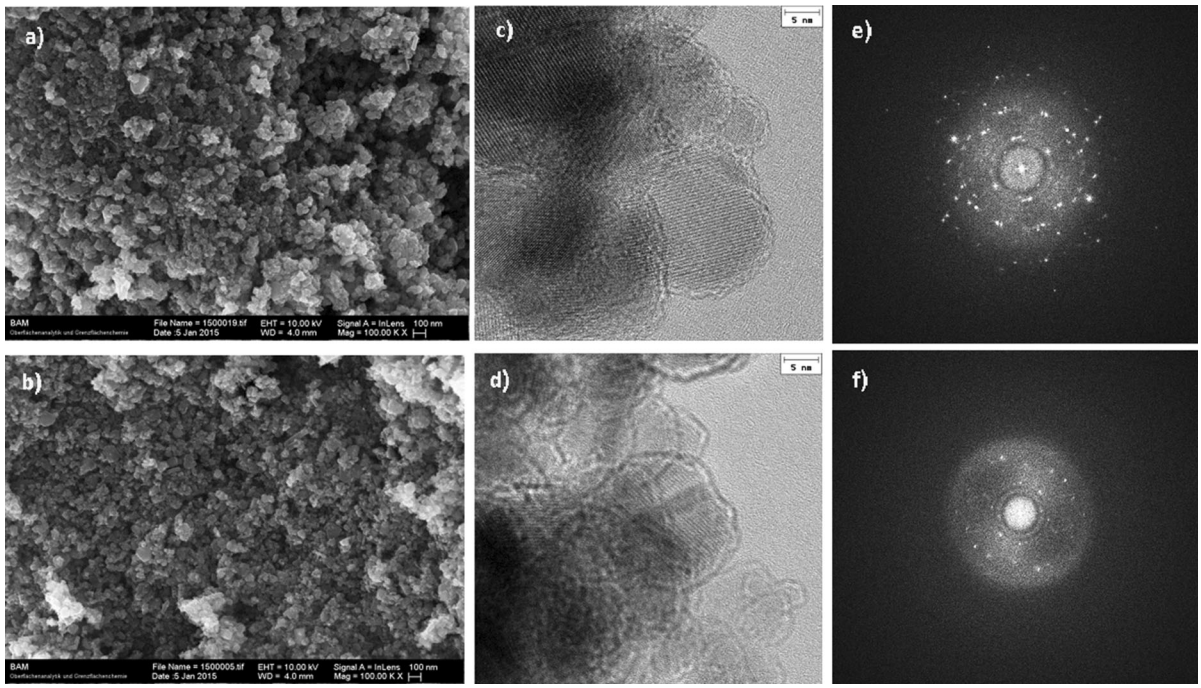

Fig. 1 SEM micrographs (*left*), HRTEM images (*middle*) together with the corresponding SAED patterns (*right*) of the Fe_3O_4-TA (*up*) and Fe_3O_4-NOM (*down*) catalysts

diffraction rings; the higher frequency of the small spots in the SAED rings in the Fe_3O_4-TA sample indicates an increased thickness of the coating layer (TA) bound on the magnetite nanoparticles compared to the Fe_3O_4-NOM sample (as is further confirmed by the FTIR analyses).

The EDX investigation at 20 kV (Fig. 2a) and 5 kV (Fig. 2b) provided more surface sensitive analysis, as well as the elemental composition of both catalysts, indicating the predominance of iron, oxygen, and carbon in the studied samples; two locations were measured for each sample, the EDX spectra being

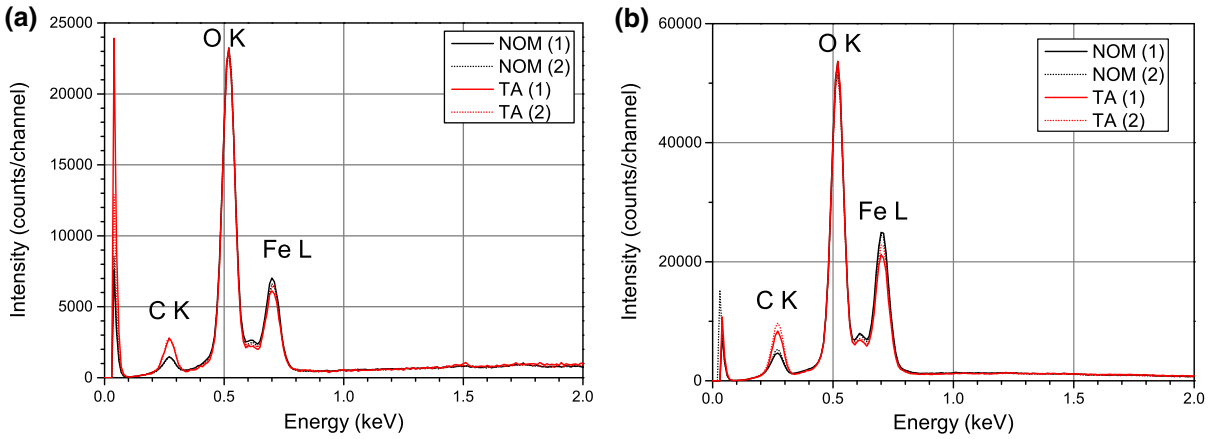

Fig. 2 EDX spectra—20 kV (**a**) and 5 kV (**b**), measured at two locations on each sample, Fe_3O_4-NOM (*black*) and Fe_3O_4-TA (*red*); the EDX spectra were normalized on the O K *line* intensity. (Color figure online)

summed up in order to get a more accurate information regarding the sample composition.

The EDX spectra were normalized to the intensity of the O K peak at 0.5 keV, in order to evaluate the differences between the two catalysts. The results at 20 kV (Fig. 2 a) were validated by EDX measurements at 5 kV (Fig. 2b) acceleration voltage. As it can be seen from Fig. 2, the Fe_3O_4-TA sample contains significantly more C and Fe (relative to O) than the Fe_3O_4-NOM sample.

FTIR measurements were carried out in order to assess the binding of the active material onto the iron oxide surface. Figure 3 a, b shows the FTIR spectra of Fe_3O_4-TA and Fe_3O_4-NOM respectively, compared to those of pure TA and NOM, and also compared to the uncoated magnetite spectral data. The FTIR bands of coated and uncoated Fe_3O_4 at wavenumbers lower than 600 cm^{-1} are ascribed to the Fe–O vibrations of iron oxide. In the Fe_3O_4-TA spectrum (Fig. 3a), the phenolic groups of TA are seen in the region $\sim$1000–1343 cm^{-1}, while the absorption bands between 1400 and 1650 cm^{-1} are related to aromatic –C=C– bonds (Atacan and Özacar 2015). In the case of pure NOM spectrum (Fig. 3b), the peaks at 1616 and 1712 cm^{-1} correspond to the stretching vibration of C=O bond in carboxylic salt and free carboxylic acid, respectively (Peng et al. 2012); these are also present in the Fe_3O_4-NOM catalyst spectrum at $\sim$1628 cm^{-1} suggesting the interaction of carboxylate group with the FeO surfaces. The FTIR measurements also reveal that TA formed stronger interactions with Fe_3O_4, compared to NOM.

Both samples exhibit good crystallinity as confirmed by XRD analysis. Figure 4 shows the XRD patterns of TA- and, respectively, NOM-coated iron oxide nanoparticles, which were found to be typical for cubic Fe_3O_4 phase with spinel structure, the peak positions being consistent with those from the standard data for magnetite.

The nitrogen adsorption–desorption isotherms corresponding to the studied catalysts are represented in Fig. 5. The pore size distributions (insets of Fig. 5a, b), determined by the BJH method, show the presence of a dominant peak in the mesoporous range (2–50 nm); the mesopores on spheres can be assigned to the interspaces of constituent particles. The pore diameter and volume for both catalysts were also determined (see Table 1).

BET measurements revealed similar values of the surface area of both sensitized nanomaterials (Table 1) consistent with those reported in the literature. Overall, the Fe_3O_4-TA catalyst is characterized by a larger surface area with larger pores than those of Fe_3O_4-NOM sample.

The above findings can also explain the higher saturation magnetization ($M_s = 68.0$ emu/g) of Fe_3O_4-NOM than that of Fe_3O_4-TA ($M_s = 58.2$ emu/g), as depicted in Fig. 6 (as a thinner shell will allow the core to exhibit enhanced magnetic properties of the nanoparticles). The obtained results are in agreement with those reported in literature for the magnetization curves of coated Fe_3O_4 recorded at room temperature (Atacan and Özacar 2015; Peng et al. 2012).

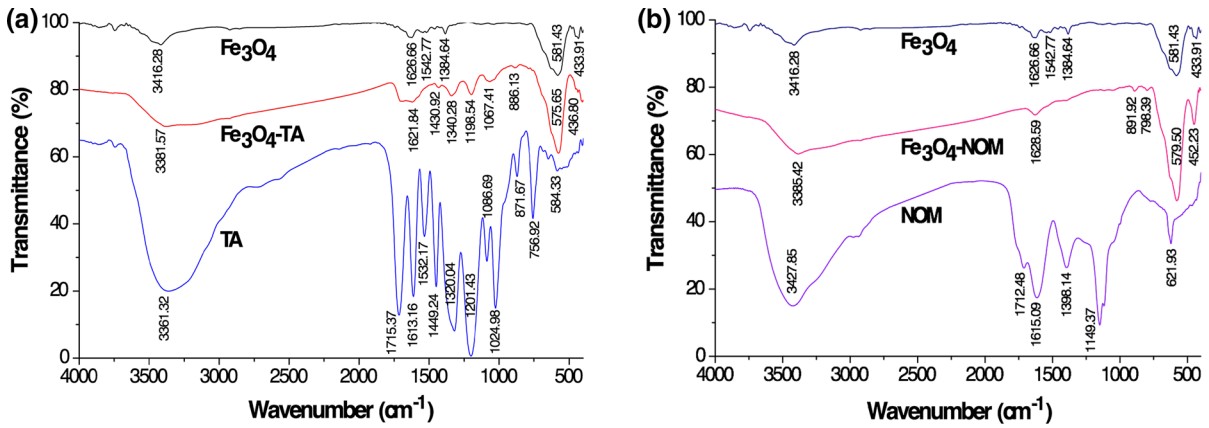

Fig. 3 FTIR spectra of uncoated Fe_3O_4, Fe_3O_4-TA, and TA (**a**); FTIR spectra of uncoated Fe_3O_4, Fe_3O_4-NOM, and NOM (**b**)

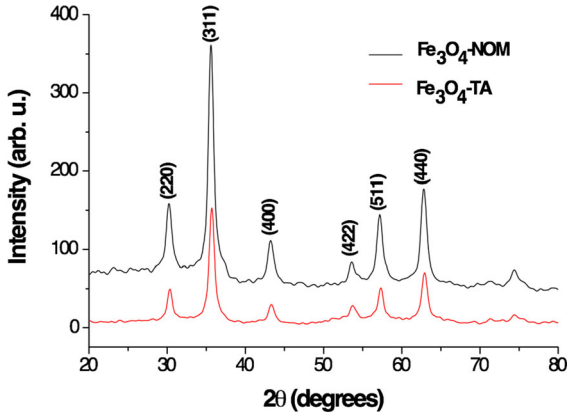

Fig. 4 The XRD patterns of Fe_3O_4-TA and Fe_3O_4-NOM samples. (Color figure online)

Following catalysts' characterization, their catalytic activity of the two resulted nanocatalysts in heterogeneous oxidation of aqueous solutions containing BPA was comparatively studied. The effects of catalyst loading, H_2O_2 dosage, and UV light on the degradation performance of the oxidation process were investigated. All catalytic experiments were carried out at laboratory scale at room temperature.

All kinetic measurements were carried out for BPA pollutant initial concentration of 0.5 μM. The (photo-) degradation experiments were performed after adsorption/desorption equilibrium between the catalysts and BPA had been reached, and monitored regularly for various reaction times (up to 120 min). Although both catalysts showed negligible adsorption of BPA onto their surface, the catalytic oxidation process revealed high removal rate of BPA as depicted in Fig. 7.

Two catalyst concentrations (1.0 and 1.5 g/L) were first tested in the aqueous BPA samples (Fig. 7a); 1.0 g/L catalyst dosage was selected for the subsequent degradation tests, since no significant increase in

Table 1 Surface properties of the studied nanocatalysts

Catalyst type	BET surface area (m^2/g)	BJH pore size (nm)	Pore volume (cm^3/g)
Fe_3O_4-TA	52.971	24.373	0.3023
Fe_3O_4-NOM	49.250	20.297	0.2499

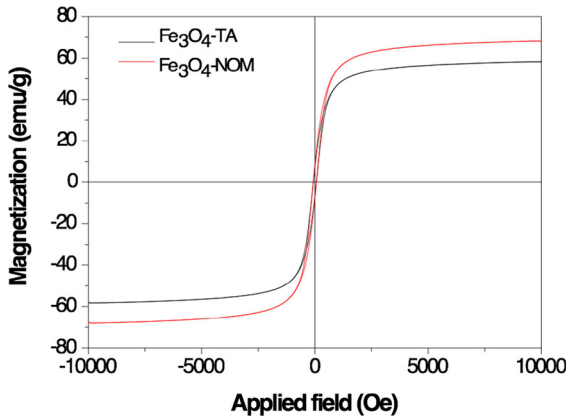

Fig. 6 Magnetization curves of the two nanocatalysts. (Color figure online)

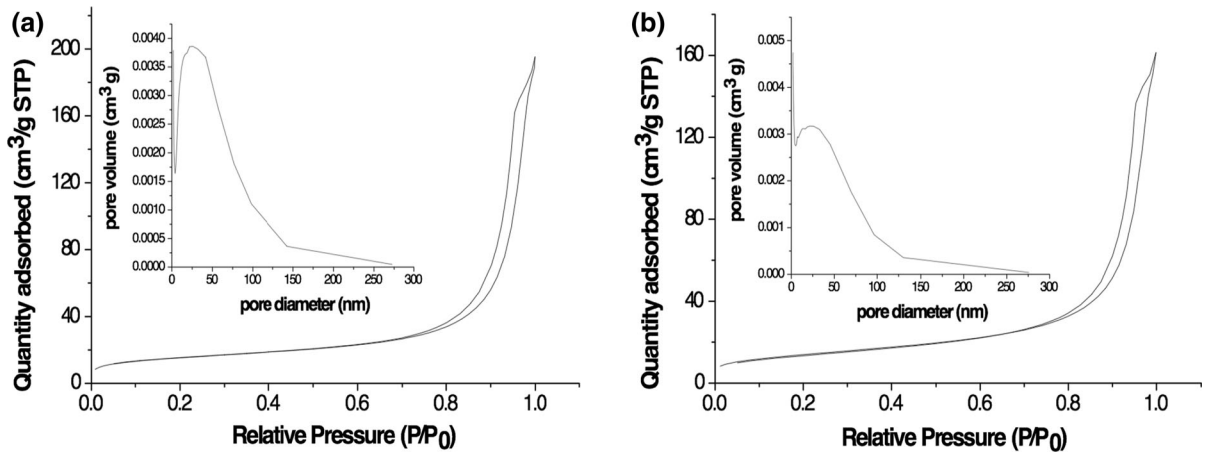

Fig. 5 The nitrogen adsorption–desorption isotherm and pore size distribution curve (*inset*) of Fe_3O_4-TA (**a**) and Fe_3O_4-NOM (**b**) catalysts

BPA removal was noticed by further increasing the catalyst dosage above 1.0 g/L.

Finding the optimum H_2O_2 concentration was also important regarding the overall efficiency of the treatment method for BPA removal from solution and minimizing operating costs in the Fenton-like oxidation using the manufactured magnetic catalysts. In solution, persistent pollutants undergo fast mineralization in the presence of low concentration of H_2O_2, in a process (heterogeneous Fenton-like oxidation) in which the generated hydroxyl radicals are oxidizing the organic contaminants by breaking them down into non-toxic products. The mechanism of reaction on the surface of iron oxide has been earlier reported by other authors (Voinov et al. 2011; Gorski et al. 2012; Pecher et al. 2002; Ai et al. 2013). It was stated that the ferrimagnetic catalysts could activate molecular oxygen via single-electron reduction pathway to produce reactive oxygen species (ROSs), including hydrogen peroxide (H_2O_2), superoxide radical ($\cdot O^{2-}$), singlet oxygen ($^1O_2$), and hydroxyl radical ($\cdot OH$), which are capable of oxidizing contaminants that cannot be removed. As it can be observed from Fig. 7b, by increasing the addition of hydrogen

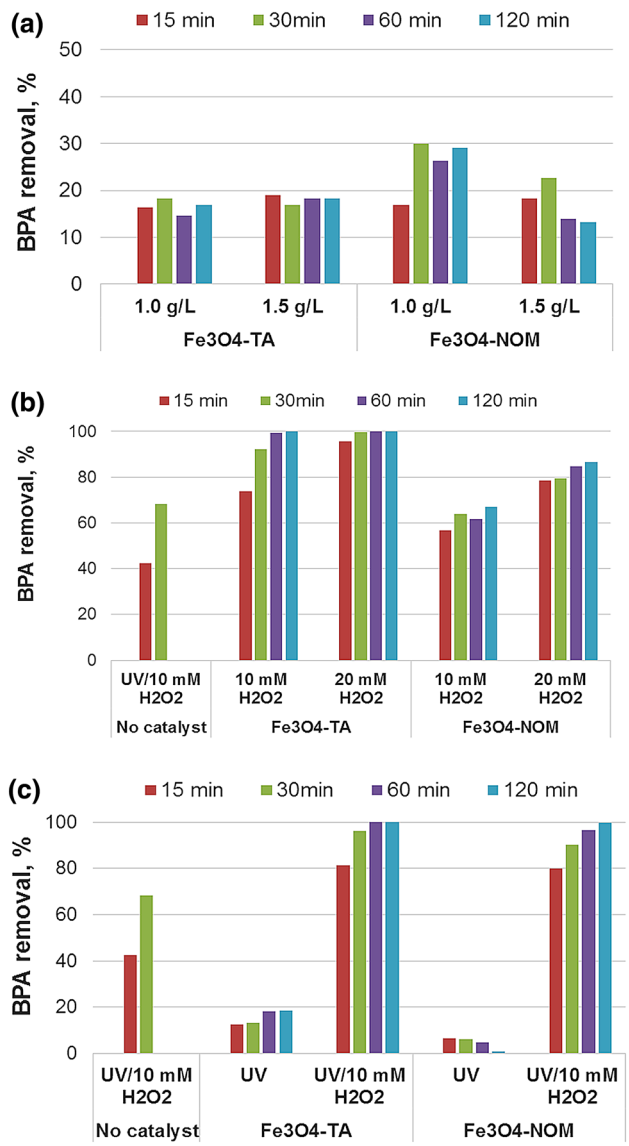

Fig. 7 The effect of catalyst loading (**a**), H_2O_2 dosage (**b**), and UV light (**c**) on BPA removal over the two catalysts. Initial conditions: 0.5 μM of pollutant, 1.0 g/L catalyst, and pH 6.6. (Color figure online)

peroxide in solution from 10 mM to 20 mM, the BPA is more rapidly decomposed (while keeping the other above-specified parameters involved in reaction the same). However, for the subsequent degradation tests, the 10 mM H_2O_2 concentration was chosen as the cost-effective condition to achieve high degradation of BPA in solution. The complete conversion of BPA was achieved in less than 60 min in the presence of Fe_3O_4-TA, while only 67 % BPA was removed from solution in 120 min when using the Fe_3O_4-NOM catalyst.

In addition, the removal efficiency of BPA was also monitored under simulated solar light (UVA irradiation) (Fig. 7c), since, by photo-oxidation, enhanced pollutant degradation is achieved faster; we also showed that in the absence of H_2O_2, UVA irradiation of the studied samples is hardly effective in the BPA removal process (Fig. 7b, c). By hydrogen peroxide addition in solution exposed to UVA, the catalytic oxidation is rapidly triggered and BPA decomposition is significantly accelerated in the presence of the reactive radical species generation in solution. The optimum experimental parameters were found to be 1.0 g/L of catalyst and 10 mM H_2O_2, under UV irradiation. As expected, more than 80 % of BPA were removed by each catalyst after 30 min of reaction time under the experimental conditions given above (Fig. 7c). The intermediates generated during the attack of the hydroxyl radicals have been identified in our earlier studies (Neamtu and Frimmel 2006) and by other authors (Katsumata et al. 2004). The first step involves the hydrogen abstraction. Generally, it is considered that BPA is degraded to BPA quinone, probably via catechol followed by the formation of semiquinone (Sajiki and Yonekubo 2003). Based on the results obtained by other researchers, 4-isopropylphenol, *p*-hydroquinone, 4-(1-hydroxy-1-methylethyl)-phenol, and phenol are formed by attack of hydroxyl radicals. Furthermore, an oxidative ring-opening reaction leads to the formation of aliphatic compounds and finally to CO_2.

One important advantage of magnetic catalysts is that they can be easily recovered from the reaction medium, recycled, and further used in subsequent catalytic oxidation cycles. The reusability tests for both catalysts were examined under the same optimal conditions. The catalysts were easily recovered from solution using a permanent magnet and rinsed several times with deionized water, being further used to evaluate their stability and catalytic efficiency in a second cycle of BPA mineralization. As shown in Fig. 8, after the second run, the catalysts are recyclable and maintain their stability; nearly 70 % of BPA was degraded in the case of Fe_3O_4-TA and, respectively, 64 % for Fe_3O_4-NOM catalyst, suggesting that both reused catalysts maintain good activity.

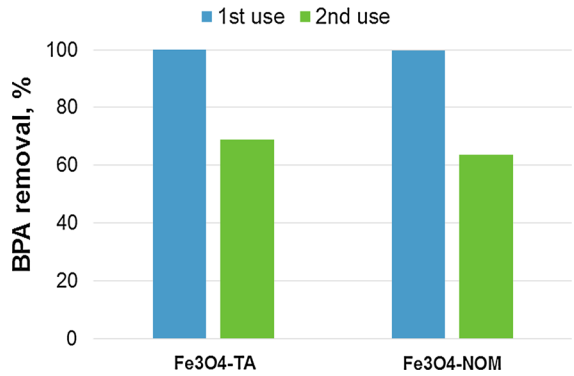

Fig. 8 Stability and reusability tests of the two catalysts. Initial conditions: 0.5 μM of pollutant, 1.0 g/L catalyst, 10 mM H_2O_2, pH 6.6, and reaction time 2 h. (Color figure online)

The above results clearly showed the best overall performance of the Fe_3O_4-TA material, while Fe_3O_4-NOM exhibited a significantly lower reactivity compared to Fe_3O_4-TA. Since the surface properties of the catalysts were found to be roughly similar, we could assume that their differences in reactivity could be due to the properties and thickness of the coating shell surrounding the magnetic iron oxide core.

Conclusion

The synthesis, characterization, and performance of two environmentally friendly magnetic catalysts were investigated at the laboratory scale in the present study. Tannic acid and dissolved NOM were the reactive materials of choice grafted on the surface of magnetite cores. We have demonstrated the Fenton-like oxidation capability of the two manufactured magnetic catalysts for complete degradation of BPA in solution under UV irradiation for 1.0 g/L of catalyst and 10 mM H_2O_2, as optimum operational parameters involved in the catalytic photo-oxidation under mild reaction conditions. The present study revealed the superior reactivity of Fe_3O_4-TA as compared to the Fe_3O_4-NOM nanocatalyst. The obtained results

showed the suitability of both catalysts for the efficient degradation of persistent pollutants in waters. Although future studies are needed in order to demonstrate the applicability and feasibility of such water treatment method at large scale, the catalytic photo-oxidation of non-biodegradable hazardous micropollutants based on magnetic nanocatalysts represents an attractive sustainable option in the management of water pollution.

Acknowledgments The authors acknowledge the financial support of the Romanian Ministry of National Education CNCS–UEFISCDI through the national grant PN-II-ID-PCE-2012-4-0477 and BAM Institute (Berlin, Germany). The authors also thank Dr. V. Nica for XRD analysis, Dr. P. Postolache for VSM measurements (Faculty of Physics, 'Alexandru Ioan Cuza' University in Iasi, Romania), and Prof. Dr. A. Pui (Faculty of Chemistry, 'Alexandru Ioan Cuza' University in Iasi, Romania) for the FTIR recordings.

Compliance with ethical standards

Conflict of Interest The authors declare that they have no conflict of interest.

References

Ai ZH, Gao Z, Zhang L, He W, Yin JJ (2013) Core-Shell structure dependent reactivity of Fe@Fe2O3 nanowires on aerobic degradation of 4-Chlorophenol. Environ Sci Technol 47:5344–5352. doi:10.1021/es4005202

Atacan K, Özacar M (2015) Characterization and immobilization of trypsin on tannic acid modified Fe_3O_4 nanoparticles. Coll Surf B 128:227–236. doi:10.1016/j.colsurfb.2015.01.038

Chong MN, Jin B, Chow CWK, Saint C (2010) Recent developments in photocatalytic water treatment technology: a review. Water Res 44:2997–3027. doi:10.1016/j.watres.2010.02.039

Defoin A, Defoin-Straatmenn R, Hildenbrand K, Bittersmann E, Kreft D, Kühn HJ (1986) A new liquid phase actinometer: quantum yield and photo-CIDNP study of phenylglyoxylic acid in aqueous solution. J. Photochem 33:237–255

Genuino HC, Mazrui N, Seraji MS, Luo Z, Hoag GE (2013) Green synthesis of iron nanomaterials for oxidative catalysis of organic environmental pollutants. Chapter 3. In: New and future developments in catalysis. pp 41–61

Gilmour CR (2012) Water treatment using advanced oxidation processes: application perspectives. Dissertation. University of Western Ontario-Electronic Thesis and Dissertation Repository. Paper 836

Gorski CA, Handler RM, Beard BL, Pasararnis T, Johnson CM, Scherer MM (2012) Fe atom exchange between aqueous Fe^{2+} and magnetite. Environ Sci Technol 46:12399–12407. doi:10.1021/es204649a

Hanif S, Shahzad A (2014) Removal of chromium(VI) and dye Alizarin Red S (ARS) using polymer-coated iron oxide (Fe_3O_4) magnetic nanoparticles by co-precipitation method. J Nanopart Res 16:2429. doi:10.1007/s11051-014-2429-8

Katsumata H, Kawabe S, Kaneco S, Suzuki T, Ohta K (2004) Degradation of Bisphenol A in water by the photo-Fenton reaction. J Photochem Photobiol A 162:297–305. doi:10.1016/S1010-6030(03)00374-5

Liu JF, Zhao ZS, Jiang GB (2008) Coating Fe_3O_4 magnetic nanoparticles with humic acid for high efficient removal of heavy metals in water. Environ Sci Technol 42:6949–6954

Munoz M, de Pedro ZM, Casas JA, Rodriguez JJ (2015) Preparation of magnetite-based catalysts and their application in heterogeneous Fenton oxidation—a review. Appl Catal B 176:249–265. doi:10.1016/j.apcatb.2015.04.003

Nadejde C, Neamtu M, Hodoroaba VD, Schneider RJ, Paul A, Ababei G, Panne U (2015) Green Fenton-like magnetic nanocatalysts: synthesis, characterization and catalytic application. Appl Catal B 176–177:667–677. doi:10.1016/j.apcatb.2015.04.050

Neamtu M, Frimmel FH (2006) Degradation of endocrine disrupting bisphenol A by 254 nm irradiation in different water matrices and effect on yeast cells. Water Res 40:3745–3750. doi:10.1016/j.watres.2006.08.019

Neamtu M, Grandjean D, Sienkiewicz A, Le Faucheur S, Slaveykova V, Velez Colmenares J, Pulgarín C, De Alencastro FL (2014) Degradation of eight relevant micropollutants in different water matrices by neutral photo-Fenton process under UV254 and simulated solar light irradiation—a comparative study. Appl Catal B 158–159:30–37. doi:10.1016/j.apcatb.2014.04.001

Nowack B (2008) Pollution prevention and treatment using nanotechnology. Chapter 1. In: Krug H (ed.). Nanotechnology. Volume 2: environmental aspects. Wiley-VCH Verlag GmbH & Co. KGaA, Weinheim

Pecher K, Haderlein SB, Schwarzenbach RP (2002) Reduction of polyhalogenated methanes by surface-bound Fe(II) in aqueous suspensions of iron oxides. Environ Sci Technol 36:1734–1741. doi:10.1021/es011191o

Peng L, Qin P, Lei M, Zeng Q, Song H, Yang J, Shao J, Liao B, Gu J (2012) Modifying Fe_3O_4 nanoparticles with humic acid for removal of Rhodamine B in water. J Haz Mat 209–210:193–198. doi:10.1016/j.jhazmat.2012.01.011

Qu X, Alvarez PJJ, Li Q (2013) Applications of nanotechnology in water and wastewater treatment. Water Res 47:3931–3946. doi:10.1016/j.watres.2012.09.058

Ren B, Han C, Al Anazi Ah, Nadagouda MN, Dionysiou DD (2013) Iron-based nanomaterials for the treatment of emerging environmental contaminants. Chapter 8. In: Doong R et al. (eds.). Interactions of nanomaterials with emerging environmental contaminants. ACS Symposium Series. American Chemical Society, Washington DC. doi:10.1021/bk-2013-1150.ch008

Sajiki J, Yonekubo J (2003) Leaching of bisphenol A (BPA) to seawater from polycarbonate plastics and its degradation by reactive species. Chemosphere 51:55–62. doi:10.1016/S0045-6535(02)00789-0

Shahwan T, Abu Sirriah S, Nairat M, Boyaci E, Eroglu AE, Scott TB, Hallam KR (2011) Green synthesis of iron nanoparticles and their application as a Fenton-like catalyst for the degradation of aqueous cationic and anionic

dyes. Chem Eng J 172:258–266. doi:10.1016/j.cej.2011.05.103

Song XC, Zheng YF, Yin HY (2013) Catalytic wet air oxidation of phenol over Co-doped Fe_3O_4 nanoparticles. J Nanopart Res 15:1856. doi:10.1007/s11051-013-1856-2

Sun SP, Lemley AT (2011) p-Nitrophenol degradation by a heterogeneous Fenton-like reaction on nano-magnetite: process optimization, kinetics, and degradation pathways. J Molecular Catal A 349:71–79. doi:10.1016/j.molcata.2011.08.022

Virkutyte J, Varma RS, Jegatheesan V (2010) Treatment of micropollutants in water and wastewater. IWA Publishing, London

Voinov MA, Sosa JO, Pagan S, Morrison E, Smirnova TI, Smirnov AI (2011) Surface-mediated production of hydroxyl radicals as a mechanism of iron oxide nanoparticle biotoxicity. J Am Chem Soc 133:35–41. doi:10.1021/ja104683w

Wang D, Astruc D (2014) Fast-growing field of magnetically recyclable nanocatalysts. Chem Rev 114:6949–6985. doi:10.1021/cr500134h

Wang C, Liu H, Sun Z (2012) Heterogeneous photo-Fenton reaction catalyzed by nanosized iron oxides for water treatment. Int J Photoenergy. doi:10.1155/2012/801694

Zhang J, Zhuang J, Gao L, Zhang Y, Gu N, Feng J, Yang D, Zhu J, Yan X (2008) Decomposing phenol by the hidden talent of ferromagnetic nanoparticles. Chemosphere 73:1524–1528. doi:10.1016/j.chemosphere.2008.05.050

Zhang S, Zhao X, Niu H, Shi Y, Cai Y, Jiang G (2009) Superparamagnetic Fe_3O_4 nanoparticles as catalysts for the catalytic oxidation of phenolic and aniline compounds. J Haz Mat 167:560–566. doi:10.1016/j.jhazmat.2009.01.02